PET of Aromatase in Gastric Parietal Cells Using ^{11}C-Vorozole

Makoto Ozawa[1], Kayo Takahashi[1], Ko-hei Akazawa[1], Tadayuki Takashima[1], Hiroko Nagata[2], Hisashi Doi[2], Takamitsu Hosoya[3], Yasuhiro Wada[1], Yilong Cui[4], Yosky Kataoka[4], and Yasuyoshi Watanabe[1]

[1]Molecular Probe Dynamics Laboratory, RIKEN Center for Molecular Imaging Science, Minatojima minamimachi, Chuo-ku, Kobe, Hyogo, Japan; [2]Molecular Imaging Labeling Chemistry Laboratory, RIKEN Center for Molecular Imaging Science, Minatojima minamimachi, Chuo-ku, Kobe, Hyogo, Japan; [3]Graduate School of Biomedical Science, Tokyo Medical and Dental University, Kanda-Surugadai, Chiyoda-ku, Tokyo, Japan; and [4]Cellular Function Imaging Laboratory, RIKEN Center for Molecular Imaging Science, Minatojima minamimachi, Chuo-ku, Kobe, Hyogo, Japan

Aromatase is a rate-limiting enzyme for estrogen biosynthesis and has been implicated in pathophysiological states of various diseases via estrogen production. This enzyme is known to be widely distributed in extragonadal and gonadal tissues including the stomach. In contrast to circulating estrogen, the functional role of gastric aromatase/estrogen has not been elucidated in detail, because there is no efficient methodology to investigate spatiotemporal changes of gastric aromatase/estrogen in vivo. Recently, (*S*)-^{11}C-6-[(4-chlorophenyl)(1*H*-1,2,4-triazole-1-yl)methyl]-1-methyl-1*H*-benzotriazole (^{11}C-labeled vorozole), based on a potent nonsteroidal aromatase inhibitor, has been developed as a tracer to investigate aromatase distribution in living animals and humans using a noninvasive PET technique. In the present study, we investigated gastric aromatase expression by means of PET with ^{11}C-vorozole. **Methods:** After bolus injection of ^{11}C-vorozole into the tail vein, emission scans were obtained for 90 min on male and female rats under isoflurane anesthesia. Displacement studies with unlabeled vorozole and autoradiographic analysis were conducted for demonstration of specific binding. Immunohistochemistry was performed to confirm aromatase expression. **Results:** PET scans revealed that ^{11}C-vorozole highly accumulated in the stomach and adrenal glands. Displacement studies and autoradiography demonstrated that aromatase was expressed in the stomach but that the accumulation of ^{11}C-vorozole in the adrenal glands might be through nonspecific binding. Immunohistochemical analysis revealed that aromatase is expressed in gastric parietal cells but not in adrenal glands. Moreover, the accumulation of ^{11}C-vorozole in the stomach was significantly increased in fatigued rats. **Conclusion:** These results suggest that the ^{11}C-vorozole PET technique is a useful tool for evaluation of gastric aromatase dynamics in vivo, which may provide important information for understanding the molecular mechanisms of gastric aromatase/estrogen–related pathophysiological processes and for the development of new drugs.

Key Words: positron emission tomography; gastric aromatase; ^{11}C-vorozole; fatigue

J Nucl Med 2011; 52:1964–1969
DOI: 10.2967/jnumed.110.087072

Aromatase is a key enzyme for the production of sex steroids and catalyzes the final step of the biosynthetic pathway of estrogens. Aromatase has been reported to be widely distributed in extragonadal and gonadal tissues including the ovaries (*1*), testis (*2*), placenta (*3*), adipose tissues (*4*), skin (*5*), and brain (*6*). Aromatase is well known to take part in various important functions, such as cell proliferation and differentiation, through estrogen biosynthesis in an endocrine, autocrine, or paracrine fashion (*7*). Recently, Ueyama et al., using morphological and biochemical methods, determined that parietal cells in rat gastric mucosa express aromatase and substantially secrete estrogen into the portal vein (*8,9*). Though gastric aromatase/estrogen has been implicated in several pathophysiological states, such as liver regeneration (*10*) and feminization (*11*), by acting as a local regulator of the gastrohepatic axis, the functional role of gastric aromatase/estrogen has still to be elucidated. One of the obstacles to clarification of its role is that gastric estrogen is thought to be trapped and metabolized in the liver and rarely overflows into the systemic circulation (*9*). Therefore, an adequate method for evaluation of the spatiotemporal changes in gastric aromatase/estrogen in vivo is necessary.

Noninvasive molecular imaging techniques, such as PET, provide powerful tools for quantitative investigation of the tissue-distribution and dynamic changes of functional molecules in vivo, because of their high sensitivity and spatiotemporal resolution. ^{11}C-labeled vorozole, (*S*)-^{11}C-6-[(4-chlorophenyl)(1*H*-1,2,4-triazole-1-yl)methyl]-1-methyl-1*H*-benzotriazole (*12*), was developed as a PET tracer to investigate the in vivo distribution of aromatase in living animals and humans (*13,14*). Consistent with previous reports, we have shown that the accumulation of ^{11}C-vorozole was

Received Dec. 25, 2010; revision accepted Aug. 8, 2011.
For correspondence or reprints contact: Yasuyoshi Watanabe, Molecular Probe Dynamics Laboratory, RIKEN Center for Molecular Imaging Science, 6-7-3 Minatojima minamimachi, Chuo-ku, Kobe, Hyogo 650-0047, Japan.
E-mail: yywata@riken.jp
Published online Nov. 9, 2011.

increased in several brain regions of rats and monkeys treated with anabolic steroids (*15–18*), indicating that ^{11}C-vorozole is a useful molecular probe for aromatase imaging. In the present study, we used ^{11}C-vorozole PET to evaluate gastric aromatase under physiological and pathological conditions.

MATERIALS AND METHODS

Animals

Male and female Sprague–Dawley rats, 8–9 wk old and weighing approximately 300 g, were purchased from Japan SLC, Inc. During the experiment, body temperature was maintained at 37°C. All experimental protocols were approved by the Ethics Committee on Animal Care and Use of RIKEN and were performed in accordance with the *Guide for the Care and Use of Laboratory Animals* (*19*).

Chemicals

(*S*)-^{11}C-6-[(4-chlorophenyl)(1*H*-1,2,4-triazole-1-yl)methyl]-1-methyl-1*H*-benzotriazole (^{11}C-vorozole) was synthesized from its *N*-demethylated derivative via a reaction of *N*-methylation with ^{11}C-methyl iodide (*20*). Synthesized ^{11}C-vorozole was purified using reversed-phase high-performance liquid chromatography. Specific radioactivity of ^{11}C-vorozole was 32–49 GBq/μmol, and radiochemical purity was greater than 99.5%. The solvent was removed in vacuo, and the residue was dissolved in saline for injection. Injected volume was 0.5 mL. Unlabeled vorozole was a kind gift from the Janssen Research Foundation. Letrozole was purchased from LKT Labs, Inc.

PET Scans

The rats ($n = 6$) were anesthetized and maintained using a mixture of 1.5% isoflurane and nitrous oxide/oxygen (7:3) and positioned in the PET scanner gantry (microPET Focus220; Siemens Co., Ltd.). After a bolus injection of ^{11}C-vorozole (injected radioactivity, 95–98 MBq; chemical mass, 0.7–1.5 μg per animal) into the tail vein, a 90-min emission scan was obtained. The abdominal region was scanned for up to 5 min and sorted into 60 × 5 s dynamic signograms. Whole-body scans were then obtained with 180-s duration for 1 bed pass. Emission data were acquired in the list mode. For whole-body scans, the scanner bed was moved continuously in a reciprocating motion to ensure scanning of the entire rat body, and the data were sorted into dynamic signograms for every 1 bed pass. Emission data were reconstructed by Fourier rebinning and maximum likelihood expectation maximization. For the abdominal scans, the radioactivity concentrations in the region of interest were expressed as standardized uptake value or percentage injected dose. For the whole-body scans (continuous bed-motion acquisition), the radioactivity in the region of interest was estimated by percentage of total radioactivity at each frame.

Displacement Studies

The rats were anesthetized and maintained using a mixture of 1.5% isoflurane and nitrous oxide/oxygen (7:3), and ^{11}C-vorozole (injected radioactivity, 96–100 MBq; chemical mass, 0.9–1.7 μg per animal) was administered by bolus injection into the tail vein. Fifteen minutes after ^{11}C-vorozole administration, unlabeled vorozole (100 μg/kg; $n = 3$) dissolved in 4% ethanol or vehicle ($n = 3$) was injected into the tail vein as a bolus. The abdominal region was scanned for 90 min (33 × 5, 55 × 30, and 20 × 180 s; a total of 108 frames). For the displacement studies with the other aromatase inhibitor, ^{11}C-vorozole was injected into a tail vein as a bolus in coadministration with letrozole (1 mg/kg) or vehicle.

Radiometabolite Analysis

Radiometabolite analysis of rat stomach and adrenal gland was performed. At 30 min after intravenous injection of ^{11}C-vorozole, the blood flow was terminated, and then the tissues were quickly removed and homogenized. Sample preparation and chromatographic separation was performed according to previously described procedures with slight modification (*18*).

Autoradiography

Frozen rat brains ($n = 3$), stomachs, and adrenal glands were sliced into serial coronal sections (25 μm) using a cryostat microtome, and the sections were thaw-mounted onto glass slides. Consecutive sections were preincubated at room temperature (~22°C) for 10 min in phosphate-buffered saline (pH 7.4) and incubated with 2 nM ^{11}C-vorozole in the presence or absence of unlabeled vorozole (1 μM) at room temperature for 30 min. The sections were washed for 2 min in the buffer 3 times and rapidly air-dried. The sections were exposed on imaging plates (BAS-SR-2040; Fujifilm) at room temperature for 40 min to generate the autoradiograms. FLA-7000 (Fujifilm) was used for scanning the imaging plates.

Immunohistochemistry

Rats ($n = 3$) were perfused with 4% formaldehyde buffered with 0.1 M phosphate-buffered saline under deep anesthesia. The stomach and adrenal glands were removed and further fixed in the same fixative at 4°C for 24 h. Frozen sections (10 μm thick) were prepared in a cryostat microtome and thaw-mounted on Superfrost glass slides (Matsunami Glass). The immunohistochemical staining procedure was described in the previous reports (*17*). After immunohistochemical detection, the slides were stained with hematoxylin and eosin.

Fatigue-Loading Procedure

The fatigued condition in rats was induced using the method previously established by our group (*21*). Briefly, rats (male, $n = 4$) were transferred to cages filled with water (23°C ± 1°C) to a height of 2.2 cm and kept in the water cage for 5 d. The water was changed once a day. Compared with the control group, rectal temperatures remained within the normal range in these rats during fatigue-loading, and no gastric ulcers were observed up to the end of fatigue-loading. Using this animal model of comprehensive fatigue, which encompasses both physical and mental fatigue, we previously reported a decrease in physical performance (*21*), alternation of the expression levels of peptidases in the pituitary gland (*22,23*), and significant changes in amino acid metabolism in the plasma (*24*). Such fatigue-induced changes in behavior and biochemical indicators were completely reversed after a return to ordinary conditions.

Data Analysis

All values are presented as the mean ± SEM. Two-way ANOVA with Scheffe multiple-comparison procedure was used to test for differences in temporal changes in time–activity curves between displacement and vehicle-treated groups. A 2-tailed unpaired *t* test was used to test for statistical difference in radioactivity between fatigued and control rats. The differences discussed in the text were considered to be significant at a value of P less than 0.05.

RESULTS

Whole-Body PET Studies

A representative whole-body maximum-intensity-projection image after bolus injection of ^{11}C-vorozole is shown in Figure 1. High accumulation of ^{11}C-vorozole was detected in the stomach and the adrenal glands (Fig. 1). In the female rats, the radioactivity was also observed in the ovarium (Fig. 1). Detectable ^{11}C-vorozole radioactivity was observed in the testis of male rats (data not shown). The temporal changes in radioactivity of ^{11}C-vorozole in these tissues were variable. ^{11}C-Vorozole accumulation in the stomach increased until the end of the PET scans but accumulation in other tissues reached a peak and then gradually decreased thereafter. The maximum radioactivity detected in the stomach was 4.31% of the total radioactivity (at the end of the PET scan, 90 min).

Displacement Studies

The radioactivity of ^{11}C-vorozole in the stomach immediately decreased after administration of unlabeled vorozole 15 min after bolus injection of ^{11}C-vorozole (Fig. 2A). The mean values of radioactivity in the stomach were significantly decreased in the unlabeled ligand–treated group ($P < 0.05$, 2-way ANOVA with Scheffe multiple-comparison procedure). However, radioactivity levels in the adrenal glands were not changed by administration of unlabeled vorozole (Fig. 2B). The plasma concentration–time curve showed no difference between the displacement and the control group, suggesting that the metabolic and excretion pathway had not been influenced by injection of unlabeled vorozole (Supplemental Fig. 1; supplemental materials are available online only at http://jnm.snmjournals.org). In addition, coadministration with unlabeled letrozole (1 mg/kg), the other aromatase inhibitor, decreased the distribution of the radioactivity in the stomach wall (Supplemental Fig. 2). Ex vivo autoradiographic images also confirmed that the radioactivity predominantly accumulated in the gastric gland region was drastically decreased by coadministration with letrozole, whereas that in adrenal glands was not significantly affected by the administration of letrozole (Supplemental Fig. 3).

Analysis of radiochromatograms revealed that almost 100% of the radioactivity in these tissues was derived from ^{11}C-vorozole (Fig. 3).

Autoradiography and Immunohistochemistry

Autoradiographic images of tissue sections of rat stomach, brain, and adrenal glands are shown in Figure 4. As reported previously (*14*), the binding of ^{11}C-vorozole to the brain amygdala was clearly displaced by unlabeled vorozole. In a similar fashion, the strong signal of ^{11}C-vorozole in the stomach was clearly eliminated by the addition of unlabeled vorozole. However, addition of unlabeled vorozole had no effect on the ^{11}C-vorozole signal in the adrenal glands. Immunohistochemical studies were then performed to confirm aromatase expression. The immunolocalization of aromatase in the stomach is shown

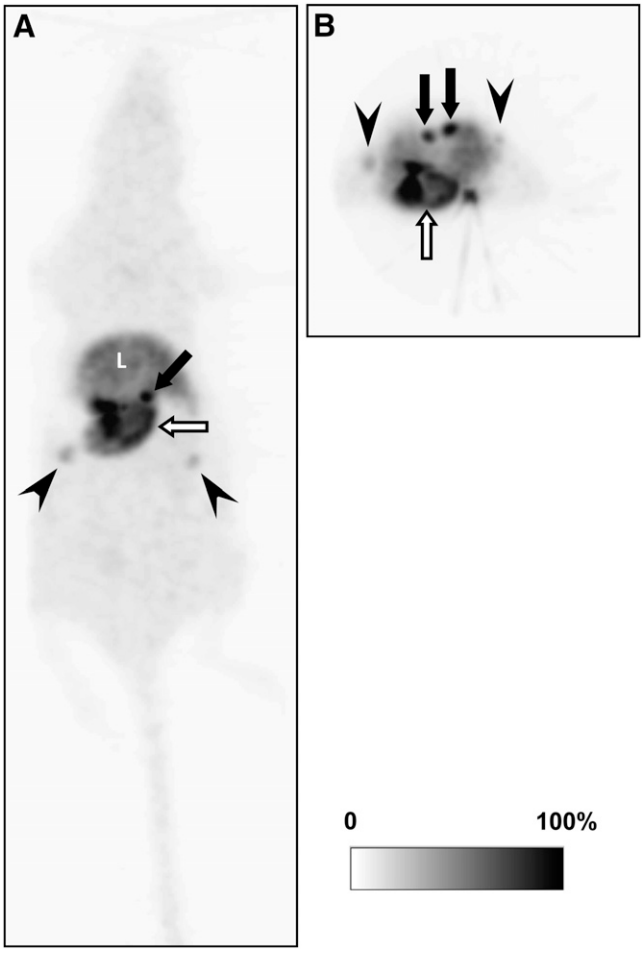

FIGURE 1. Representative whole-body maximum-intensity-projection image of ^{11}C-vorozole in female rat: coronal (A) and transverse (B) images. ^{11}C-vorozole was highly accumulated in stomach (open arrows), adrenal glands (closed arrows), and ovarium (arrowheads). L = liver.

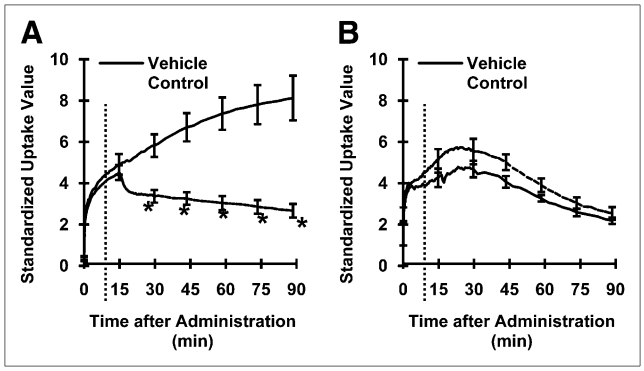

FIGURE 2. Time–activity curves for ^{11}C-vorozole displaced by excess unlabeled vorozole in stomach (A) and adrenal glands (B). Unlabeled vorozole or vehicle was administered 15 min after start of PET scans. Broken line indicates time at which unlabeled ligand was administered. Asterisks indicate significant difference ($P < 0.05$, 2-way ANOVA with Scheffe multiple-comparison procedure).

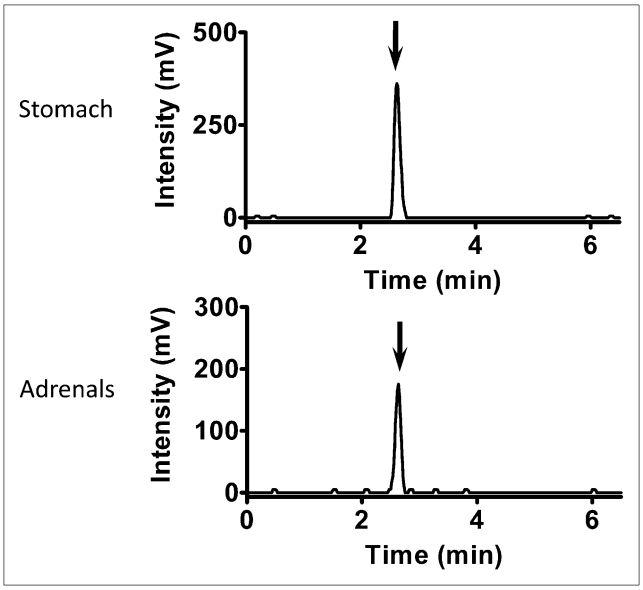

FIGURE 3. Representative high-performance liquid radiochromatograms of stomach and adrenal glands extracts after intravenous administration of ^{11}C-vorozole (~300 MBq/kg).

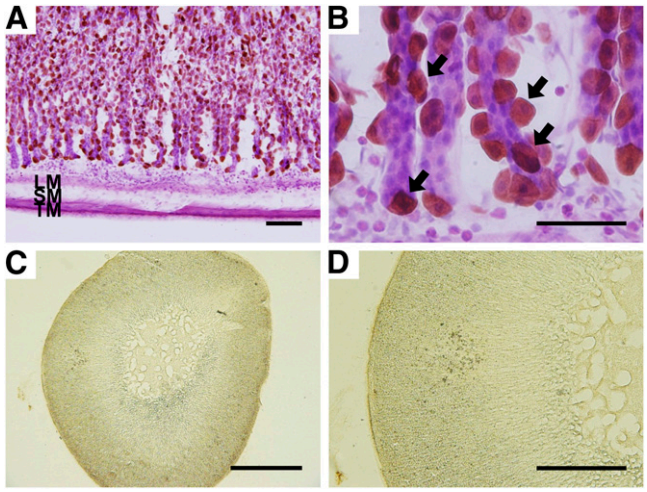

FIGURE 5. Photomicrographs of aromatase immunoreactivity in stomach and adrenal gland. Tissue sections of stomach (A and B) and adrenal gland (C and D) were analyzed for aromatase immunoreactivity. Scale bars indicate 100 μm in A, 50 μm in B, 1 mm in C, and 500 μm in D. Arrows in B indicate aromatase-immunopositive gastric parietal cells. LM = lamina muscularis mucosae; SM = submucosa; TM = tunica muscularis.

in Figure 5; aromatase immunosignals were observed in the eosinophilic cytoplasm of the gastric parietal cells that are arranged in the glandular body of fundic glands. In the adrenal glands, however, no aromatase immunosignals were detected either in the adrenal cortex or in the adrenal medulla (Fig. 5).

PET Studies in Fatigued Rats

For further investigation of the pathophysiological role of gastric aromatase, we focused on the regulatory effect of gastric estrogen on ghrelin production. Ghrelin, an endogenous ligand for the growth hormone secretagogue receptor, is predominantly produced in the stomach (*25*), and its expression and release are thought to be regulated by gastric estrogen in a paracrine fashion (*26*). Recently, ghrelin levels have been observed to be upregulated in a chronic stress model in rats (*27*), which was originally developed by our group as a comprehensive fatigue model (*21*). To confirm whether gastric aromatase is also upregulated in such a fatigued condition, we performed ^{11}C-vorozole PET studies in these fatigued rats. Consistent with our expectations, the accumulation of ^{11}C-vorozole in the stomach was increased in the fatigued group ($n = 4$), compared with the control ($n = 3$) group (Fig. 6). The radioactivity in the stomach was significantly increased in the fatigued group ($P < 0.05$, 2-tailed unpaired t test).

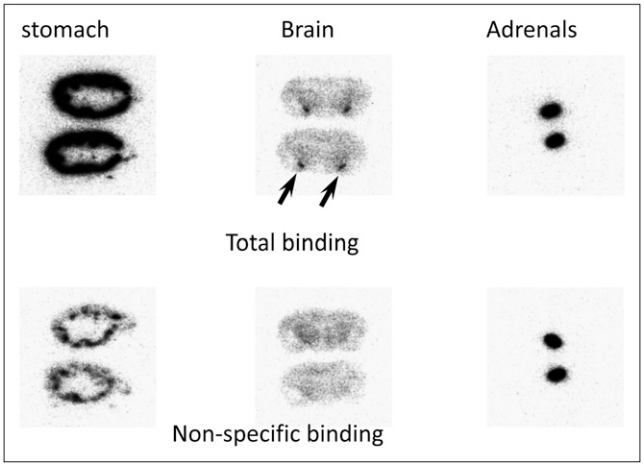

FIGURE 4. Autoradiographic images of displacement of ^{11}C-vorozole with unlabeled vorozole in tissue slices. Autoradiographic image of tissue sections of stomach, brain, and adrenal glands that were incubated with 2 nM ^{11}C-vorozole in absence (total binding) or presence (nonspecific binding) of 1 μM unlabeled vorozole. Arrows indicate amygdala.

DISCUSSION

The present study showed that aromatase is abundantly expressed in the stomach and is upregulated under conditions of severe fatigue, using an in vivo molecular imaging technique with ^{11}C-vorozole. The PET study with ^{11}C-vorozole clearly showed that the radioactivity of ^{11}C-vorozole was highly accumulated in the stomach and adrenal glands (Fig. 1). The displacement experiments performed in vivo revealed that postadministration (15 min after bolus injection of ^{11}C-vorozole) of the unlabeled compound induced a significant decrease in the level of radioactivity in the stomach but not in that in the adrenal glands (Fig. 2). The radioactivity in the stomach and adrenal glands was derived from ^{11}C-vorozole (Fig. 3). Considering the fact that vorozole inhibits aromatase activity by rever-

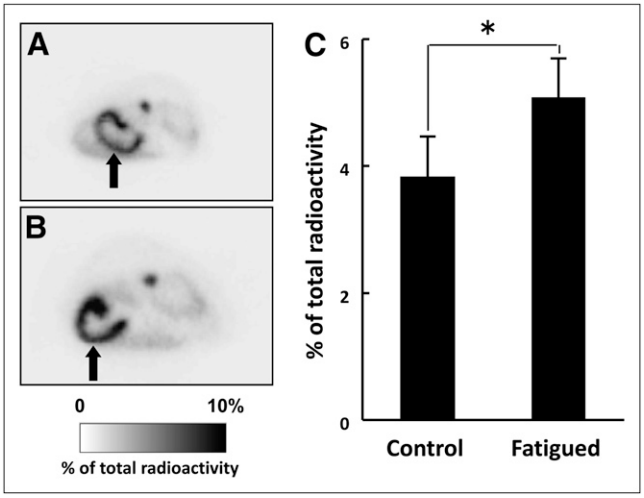

FIGURE 6. ^{11}C-vorozole radioactivity levels are increased in stomach of fatigued rat. Representative transverse image of ^{11}C-vorozole in control (A) and fatigued (B) rats from 5 to 90 min after bolus injection of ^{11}C-vorozole. Closed arrow indicates stomach. (C) ^{11}C-vorozole accumulation in stomach of control (n = 3) and fatigued (n = 4) rats. Asterisk indicates a significant difference ($P < 0.05$, 2-tailed unpaired t test).

sibly binding to its heme domain (*28,29*), these results strongly suggest that the accumulation of ^{11}C-vorozole in the stomach, but not in the adrenal glands, reflects the specific binding. These results were further supported by the in vitro autoradiographic analysis (Fig. 4). Moreover, the immunohistochemical and morphological studies also demonstrated that aromatase immunoreactivity was abundantly observed in the cytoplasm of gastric parietal cells (Fig. 5). Recently, Ueyama et al. (*8,9*), using immunohistochemistry and in situ hybridization, reported that aromatase messenger RNA and protein are localized in gastric parietal cells. They further noted that the production of estrone and 17β-estradiol from androstenedione in the gastric mucosa of the rat stomach might be catalyzed by endogenous aromatase that is localized in the stomach (*8*). The combined observations suggest that endogenous aromatase is expressed in gastric parietal cells and that the ^{11}C-vorozole PET technique is a powerful tool for noninvasive evaluation of gastric aromatase.

The second major finding of the present study is that the level of ^{11}C-vorozole radioactivity was significantly increased in the stomach of the fatigued rat, indicating upregulation of gastric aromatase under this pathological condition. Although a functional role for gastric aromatase and estrogen has not been elucidated in detail, a regulatory effect of gastric estrogen on ghrelin production has been proposed by Sakata et al. (*26*). Ghrelin, an endogenous ligand for the growth hormone secretagogue receptor, is known to be predominantly produced in the stomach (*25*). Sakata et al. demonstrated that ghrelin-producing cells are located close to gastric parietal cells and that gastric estrogen directly induces ghrelin production (*26*). Ghrelin plays important roles in growth regulation and energy homeostasis such as in stimulation of growth hormone release, in food intake, and in adiposity (*30,31*). The plasma level of ghrelin is known to be increased in response to energy insufficiency and subsequently induces a potent feeding response via activation of the growth hormone secretagogue receptor (*32*). In our fatigued model, the rat was kept in a water cage for 5 d to induce psychological and physical exhaustion, during which energy consumption would be increased. Indeed, an increase in plasma ghrelin levels has been reported in these fatigued rats (*27*). These observations suggest that an increase in gastric aromatase might be involved in energy homeostasis via regulation of gastric ghrelin production. However, the detailed mechanism of such regulation remains to be investigated.

Some recent reports noted that aromatase is localized in the adrenal glands. Conley et al. (*33*) reported that aromatase is expressed in the adrenal glands of fetal and newborn pigs. In their report, aromatase was detected in the adrenal cortex using immunohistochemistry. Illera et al. (*34*) reported that aromatase was distributed in the rat adrenal medulla, based on immunohistochemical analysis. However, using messenger RNA analysis, Ueyama et al. (*8,9*) detected no expression of the aromatase gene in rat adrenal glands. In the present study, an obvious accumulation of ^{11}C-vorozole was observed in adrenal glands. However, this accumulation of ^{11}C-vorozole was not displaced by unlabeled vorozole either in vitro or in vivo. The present immunohistochemical studies were also unable to detect aromatase immunoreactivity in adrenal glands. These results suggest that ^{11}C-vorozole might nonspecifically bind to molecules other than aromatase in adrenal glands.

Because of the beneficial effect of aromatase inhibitor treatment for estrogen-related diseases, several aromatase inhibitor compounds have been widely used as therapeutic agents (*35,36*). For instance, aromatase inhibitors have been used for the treatment of breast cancer in postmenopausal women, in which the inhibitor target is aromatase that is expressed by the breast cancer (*28*). To date, gastric aromatase has not attracted much attention in terms of drug development targeted toward estrogen-related disease. However, it is known that one of the most common adverse events of aromatase inhibitors is gastrointestinal disorders, such as nausea, vomiting, and anorexia (*37,38*). The present study clearly demonstrated that aromatase is abundantly expressed in gastric parietal cells and interacted with ^{11}C-vorozole that was administrated intravenously. Obviously, gastric aromatase is not the target of breast cancer; an inadequate inhibition of gastric aromatase is not desirable for preventing adverse effects of aromatase inhibitors. These observations suggest that development of a technology such as ^{11}C-vorozole PET that can evaluate gastric aromatase/estrogen levels is necessary for drug development targeted toward estrogen-related diseases.

CONCLUSION

This study is the first time to evaluate gastric aromatase in vivo using quantitative PET with ^{11}C-vorozole and showed that aromatase is abundantly expressed in the stomach and is upregulated in the fatigued rat. These results suggest that ^{11}C-vorozole PET enables noninvasive investigation of aromatase dynamics in vivo, possibly providing important information for understanding the functional role of gastric aromatase/estrogen in the pathophysiological process and for the development of new drugs targeted toward estrogen-related diseases.

DISCLOSURE STATEMENT

The costs of publication of this article were defrayed in part by the payment of page charges. Therefore, and solely to indicate this fact, this article is hereby marked "advertisement" in accordance with 18 USC section 1734.

ACKNOWLEDGMENTS

This work was supported in part by consignment expenses from the Molecular Imaging Program on Research Base for Exploring New Drugs from the Ministry of Education, Culture, Sports, Science, and Technology (MEXT), Japanese Government. No other potential conflict of interest relevant to this article was reported.

REFERENCES

1. el-Maasarany S, Brandt ME, Majercik MH, Zimniski SJ, Puett D. Immunocytochemical localization and enzymatic distribution of rat ovarian aromatase. *Biol Reprod.* 1991;44:550–560.
2. Brodie A, Inkster S. Aromatase in the human testis. *J Steroid Biochem Mol Biol.* 1993;44:549–555.
3. Inkster SE, Brodie AM. Immunocytochemical studies of aromatase in early and full-term human placental tissues: comparison with biochemical assays. *Biol Reprod.* 1989;41:889–898.
4. Mahendroo MS, Mendelson CR, Simpson ER. Tissue-specific and hormonally controlled alternative promoters regulate aromatase cytochrome P450 gene expression in human adipose tissue. *J Biol Chem.* 1993;268:19463–19470.
5. Leshin M, Baron J, George FW, Wilson JD. Increased estrogen formation and aromatase activity in fibroblasts cultured from the skin of chickens with the Henny feathering trait. *J Biol Chem.* 1981;256:4341–4344.
6. Roselli CE, Abdelgadir SE, Ronnekleiv OK, Klosterman SA. Anatomic distribution and regulation of aromatase gene expression in the rat brain. *Biol Reprod.* 1998;58:79–87.
7. Simpson E, Rubin G, Clyne C, et al. Local estrogen biosynthesis in males and females. *Endocr Relat Cancer.* 1999;6:131–137.
8. Ueyama T, Shirasawa N, Ito T, Tsuruo Y. Estrogen-producing steroidogenic pathways in parietal cells of the rat gastric mucosa. *Life Sci.* 2004;74:2327–2337.
9. Ueyama T, Shirasawa N, Numazawa M, et al. Gastric parietal cells: potent endocrine role in secreting estrogen as a possible regulator of gastro-hepatic axis. *Endocrinology.* 2002;143:3162–3170.
10. Francavilla A, Polimeno L, DiLeo A, et al. The effect of estrogen and tamoxifen on hepatocyte proliferation in vivo and in vitro. *Hepatology.* 1989;9:614–620.
11. Braunstein GD. Aromatase and gynecomastia. *Endocr Relat Cancer.* 1999;6:315–324.
12. Wouters W, Snoeck E, De Coster R. Vorozole, a specific non-steroidal aromatase inhibitor. *Breast Cancer Res Treat.* 1994;30:89–94.
13. Biegon A, Kim SW, Alexoff DL, et al. Unique distribution of aromatase in the human brain: in vivo studies with PET and [N-methyl-^{11}C]vorozole. *Synapse.* 2010;64:801–807.
14. Takahashi K, Bergstrom M, Frandberg P, Vesstrom EL, Watanabe Y, Langstrom B. Imaging of aromatase distribution in rat and rhesus monkey brains with [^{11}C]vorozole. *Nucl Med Biol.* 2006;33:599–605.
15. Roselli CE. The effect of anabolic-androgenic steroids on aromatase activity and androgen receptor binding in the rat preoptic area. *Brain Res.* 1998;792:271–276.
16. Takahashi K, Hallberg M, Magnusson K, et al. Increase in [^{11}C]vorozole binding to aromatase in the hypothalamus in rats treated with anabolic androgenic steroids. *Neuroreport.* 2007;18:171–174.
17. Takahashi K, Tamura Y, Watanabe Y, Langstrom B, Bergstrom M. Alteration in [^{11}C]vorozole binding to aromatase in neuronal cells of rat brain induced by anabolic androgenic steroids and flutamide. *Neuroreport.* 2008;19:431–435.
18. Takahashi K, Onoe K, Doi H, et al. Increase in hypothalamic aromatase in macaque monkeys treated with anabolic-androgenic steroids: PET study with [^{11}C]vorozole. *Neuroreport.* 2011;22:326–330.
19. *Guide for the Care and Use of Laboratory Animals.* Bethesda, MD: National Institutes of Health; 1985. NIH publication 85-23.
20. Kim SW, Biegon A, Katsamanis ZE, et al. Reinvestigation of the synthesis and evaluation of [N-methyl-^{11}C]vorozole, a radiotracer targeting cytochrome P450 aromatase. *Nucl Med Biol.* 2009;36:323–334.
21. Tanaka M, Nakamura F, Mizokawa S, Matsumura A, Nozaki S, Watanabe Y. Establishment and assessment of a rat model of fatigue. *Neurosci Lett.* 2003;352:159–162.
22. Ogawa T, Kiryu-Seo S, Tanaka M, et al. Altered expression of neprilysin family members in the pituitary gland of sleep-disturbed rats, an animal model of severe fatigue. *J Neurochem.* 2005;95:1156–1166.
23. Ogawa T, Shishioh-Ikejima N, Konishi H, et al. Chronic stress elicits prolonged activation of alpha-MSH secretion and subsequent degeneration of melanotroph. *J Neurochem.* 2009;109:1389–1399.
24. Jin G, Kataoka Y, Tanaka M, et al. Changes in plasma and tissue amino acid levels in an animal model of complex fatigue. *Nutrition.* 2009;25:597–607.
25. Kojima M, Hosoda H, Date Y, Nakazato M, Matsuo H, Kangawa K. Ghrelin is a growth-hormone-releasing acylated peptide from stomach. *Nature.* 1999;402:656–660.
26. Sakata I, Tanaka T, Yamazaki M, Tanizaki T, Zheng Z, Sakai T. Gastric estrogen directly induces ghrelin expression and production in the rat stomach. *J Endocrinol.* 2006;190:749–757.
27. Ochi M, Tominaga K, Tanaka F, et al. Effect of chronic stress on gastric emptying and plasma ghrelin levels in rats. *Life Sci.* 2008;82:862–868.
28. Brodie AM. Aromatase inhibitors in the treatment of breast cancer. *J Steroid Biochem Mol Biol.* 1994;49:281–287.
29. Wiseman LR, Spencer CM. Vorozole. *Drugs Aging.* 1997;11:245–250; discussion 251–252.
30. Tschöp M, Smiley DL, Heiman ML. Ghrelin induces adiposity in rodents. *Nature.* 2000;407:908–913.
31. Wren AM, Small CJ, Ward HL, et al. The novel hypothalamic peptide ghrelin stimulates food intake and growth hormone secretion. *Endocrinology.* 2000;141:4325–4328.
32. Zigman JM, Elmquist JK. Minireview: from anorexia to obesity—the yin and yang of body weight control. *Endocrinology.* 2003;144:3749–3756.
33. Conley AJ, Corbin CJ, Hinshelwood MM, et al. Functional aromatase expression in porcine adrenal gland and testis. *Biol Reprod.* 1996;54:497–505.
34. Illera JC, Pena L, Martinez-Mateos MM, et al. The effect of long-term exposure to combinations of growth promoters in Long Evans rats: part 2. Adrenal morphology (histopathology and immunochemical studies). *Anal Chim Acta.* 2007;586:252–258.
35. Goss PE. Pre-clinical and clinical review of vorozole, a new third generation aromatase inhibitor. *Breast Cancer Res Treat.* 1998;49(suppl 1):S59–65; discussion S73–77.
36. Tominaga T, Adachi I, Sasaki Y, et al. Double-blind randomised trial comparing the non-steroidal aromatase inhibitors letrozole and fadrozole in postmenopausal women with advanced breast cancer. *Ann Oncol.* 2003;14:62–70.
37. Muss HB, Tu D, Ingle JN, et al. Efficacy, toxicity, and quality of life in older women with early-stage breast cancer treated with letrozole or placebo after 5 years of tamoxifen: NCIC CTG intergroup trial MA.17. *J Clin Oncol.* 2008;26:1956–1964.
38. Smith IE, Walsh G, Skene A, et al. A phase II placebo-controlled trial of neoadjuvant anastrozole alone or with gefitinib in early breast cancer. *J Clin Oncol.* 2007;25:3816–3822.